International Journal of Mechanical, Industrial and Aerospace Sciences
ISSN: 2517-9950
Vol:10, No:6, 2016

Internal Power Recovery in Cryogenic Cooling Plants Part I: Expander Development

Ambra Giovannelli, Erika Maria Archilei

Abstract**—**The amount of the electrical power required by refrigeration systems is relevant worldwide. It is evaluated in the order of 15% of the total electricity production taking refrigeration and air-conditioning into consideration. For this reason, in the last years several energy saving techniques have been proposed to reduce the power demand of such plants. The paper deals with the development of an innovative internal recovery system for cryogenic cooling plants. Such a system consists in a Compressor-Expander Group (CEG) designed on the basis of the automotive turbocharging technology. In particular, the paper is focused on the design of the expander, the critical component of the CEG system. Due to the low volumetric flow entering the expander and the high expansion ratio, a commercial turbocharger expander wheel was strongly modified. It was equipped with a transonic nozzle, designed to have a radially inflow full admission. To verify the performance of such a machine and suggest improvements, two different set of nozzles have been designed and modelled by means of the commercial Ansys-CFX software. steady-state 3D CFD simulations of the second-generation prototype are presented and compared with the initial ones.

Keywords**—**Energy saving, organic fluids, radial turbine, refrigeration plant, vapor compression systems.

I. Introduction

VAPOR Compression Refrigeration (VCR) systems are commonly used in industrial and service sectors in addition to the domestic one [1]. They are large electricity consumers worldwide [2]. Therefore, in the last decades, many efforts have been spent to apply energy saving concepts to such a field. In order to reduce VCR consumptions, many solutions have been proposed improving the system control [3], [4], retrofitting the refrigeration plant [5], or, in some cases, modifying the basic cycle concept. Among them, it is possible to mention the adoption of ejector loops [5], [6], the proposal of a multistage compression process [7], the replacement of the throttling valve with an expander [8]. Many patents can be included in this field. Such patents suggest various modifications of the basic VCR system layout to allow an internal recovery [9]-[16].

The present work is related to the development of a device for internal power recovery based on Ascani's patent [17].

A. Giovannelli is with the Department of Engineering, Roma TRE University, Via della Vasca Navale 79, Rome, Italy (phone: 0039-06-57333424; fax: 0039-06-***; e-mail: ambra.giovannelli@uniroma3.it).

E.M. Archilei is with the Department of Engineering, Roma TRE University, Via della Vasca Navale 79, Rome, Italy (e-mail: erikamaria.archilei@uniroma3.it).

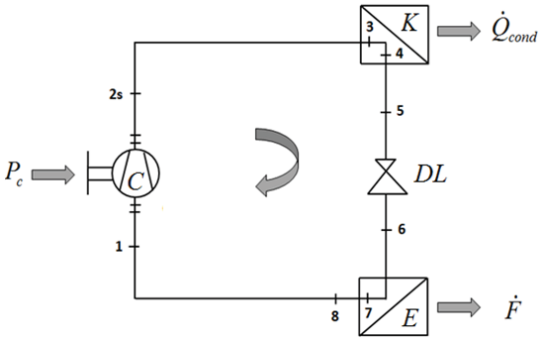

Fig. 1 VCR simple layout

II. Reference Plant

Large VCR plants are based on the concept of vapor compression inverse cycles. A basic layout is shown in Fig. 1. The plant scheme is made up of:

- An Evaporator (E), which allow the heat extraction from a heat source at low temperature. The working fluid usually evaporates completely during this transformation and it can be also slightly overheated;
- A Main Compressor (C) which gives mechanical power to the working fluid that passes from a low pressure plant section to a higher pressure one;
- A Condenser (K) for the cooling and the condensation of the working fluid by means of the rejection of thermal power to an external heat sink;
- A throttling valve (DL) which separates the plant sections at high and low pressure, adjusting the mass flow.

Performance of such plants are, usually, summarized through global quantities, as the Coefficient of Performance (COP). It is defined, under steady-state operating conditions, as the ratio between the system refrigerating capacity (the thermal power extracted from the low temperature external source) and the total mechanical power imputed in the system (given by the main compressor C).

$$COP = \frac{\dot{F}}{P_C} \tag{1}$$

As reported in Table I, the basic plant COP is close to 1. Reference boundary conditions are: evaporation temperature Te = -40 °C, condensation temperature Tc = +40 °C, overheating and subcooling ΔT_{sh} = 5 °C, ΔT_{sc} = 5 °C respectively. The reference refrigerant working fluid is R404a.

Ascani [17] proposed cycle improvements adopting an internal recovery system. Based on such starting concept, a 100 kWc Cryogenic Plant was analyzed and optimized.

Methodologies and results are extensively reported in [18]. In Fig. 2, a scheme of the modified plant layout is reported. Comparing it with the simple one in Fig. 1, two bleeds have been added in the primary flow before the throttling valve (stations marked as 5 and 6 in Fig. 2). A certain amount of liquid is extracted and heated in two heat exchangers. Once evaporated, the first one enters the expander (component EX) and, then, exhausts in the main flow before going into the Main Compressor. In such a configuration, the expander mechanical power is used for a pre-compression of the main flow, reducing the main compressor power demand. The liquid extracted with the second bleed, after the pre-heating, goes directly into the main flow entering the Main Compressor.

Table I summarizes the comparison of the global performance quantities between traditional and new configuration. Moreover, Table I together with Fig. 3, shows mass flow of the bleeds and the boundary conditions from the plant optimization process, relevant for the design of CEG components.

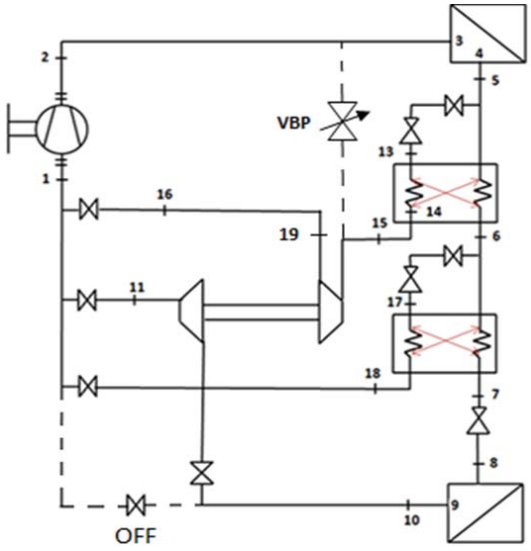

Fig. 2 VCR layout with internal recovery

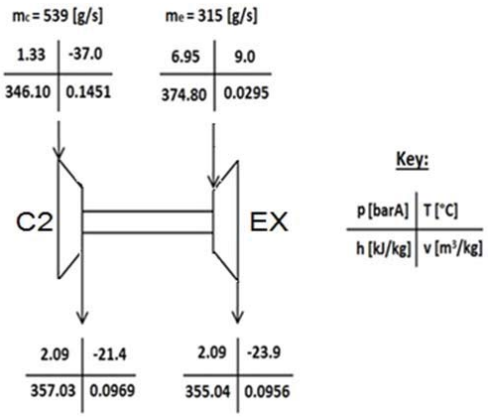

Fig. 3 CEG optimized thermodynamic and flow data

TABLE I
COMPARISON BETWEEN 100 KW SIMPLE CYCLE AND OPTIMIZED CYCLE WITH INTERNAL RECOVERY

	Simple Cycle (A)	Cycle with internal regeneration (B)	(B-A)/B [%]
F [kW]	100.00	100.00	0
Pc [kW]	101.50	74.98	-26
COP	0.98	1.33	36
Δh_{ce} [kJ/kg]	84.18	178.20	112
Mmc [kg/s]	1.19	1.05	-12
Mb1 [kg/s]		0.31	
Mc2 [kg/s]		0.56	
Mb2 [kg/s]		0.18	

III. Machinery Selection

In order to design the CEG, positive displacement machines and turbomachines have been taken into consideration for a preliminary machinery architecture selection. At the end, the adoption of machines from automotive turbocharging technology has been decided, based on compactness, availability, reliability, high performance and low cost considerations.

The preliminary selection of the reference machine has been made taking similarity rules into consideration [19], [20].

As reported in literature [21], [22] it is well known that turbomachine performance can be evaluated as functions of a certain number of independent variables. In a non-dimensional form, the pressure ratio (p0out/p0in) and the efficiency η can be expressed as function of four non/dimensional groups. In [21] the relationship is expressed as:

$$\frac{p_{0out}}{p_{0i_n}}, \eta = f\left(\frac{\rho V\sqrt{\gamma RT_{0in}}}{D^2 p_{0in}}, \frac{ND}{\sqrt{\gamma RT_{0in}}}, Re, \gamma\right) \quad (2)$$

being the first independent non-dimensional group the flow capacity and the second one the blade Mach number. Working with R404a, Mach number preservation (in the expander the R404a Mach number is around 25% of the Mach number when the expander runs with turbocharging exhaust gas) and the high Reynolds number make sufficient a simplified relationship among non/dimensional machine performance and just two non/dimensional groups. Moreover, as reported in [18], having information for technologies commercially available which correlate performance with such non/dimensional groups, a further simplification of (2) is possible:

$$\frac{p_{0out}}{p_{0in}}, \eta = f\left(\frac{NV^{\frac{1}{2}}}{\Delta h_0^{\frac{3}{4}}}, \frac{D\Delta h_0^{\frac{1}{4}}}{V^{\frac{1}{2}}}\right) = f(\omega s, Ds) \quad (3)$$

Such information has been implemented in the tool developed for the cycle optimization. In such a way, once the cycle layout has been established, the optimization process can give the optimum of the cycle parameters together with the selection of machines for a preliminary design.

The expander has been identified as the critical CEG component. In order to address the new requirements, a turbocharger expander wheel has been strongly modified and

equipped with variable nozzles, designed to have a radially inflow full admission. To verify the performance of such a machine and suggest improvements, a numerical fluid dynamic model has been set up for two set of nozzle blades. Simulations have been carried out for various radial arrangements around the rotor as reported in the next paragraphs.

IV. Expander

According to the optimization process results, the selection of the basic commercial expander wheel has been carried on taking the transmitted torque into consideration. Once the proper shaft stem was selected, the corresponding expander wheel was fixed consequently, because generally turbochargers have the expander wheel welded with the shaft. In such a way a Garrett 3582 wheel was selected and then modified reducing the blade height in order to address the proper expected fluid dynamic conditions. Moreover, the rotor was equipped with nozzle vanes to reach the expected velocities and flow angles at the rotor inlet [19], [20].

Some issues occurred for the preliminary design of the nozzle blades because the dynamic behavior in transonic conditions of the working fluid R404a (a mixture of several fluids with different physical properties), is not well known.

Thus, the following procedure was adopted:

1. Design the first prototype equipping it with supersonic convergent-divergent shape nozzle blades on the basis of the known R404a properties [23];
2. Model and analyze the first prototype geometry by means of CFD methods;
3. Build the first prototype and test it on an “air test bench” at University of Roma Tre laboratories;
4. Compare CFD simulations and test results for the first prototype operated with air;
5. On the basis of the comparison response, modify or not the prototype. If the results are sufficiently satisfying, model and analyze the prototype, replacing air with R404a.
6. Test the prototype on a test bench, built “ad-hoc” at Angelantoni Industries S.p.A.;
7. Compare CFD and test results, validating the model with R404a and suggesting useful prototype modifications.
8. Modify the preliminary geometry according to the acquired information;
9. Model and analyze by means of CFD methods the new geometry;
10. Improve the preliminary prototype geometry to build a new one.

Steps 1-7 had been already addressed and shown in [18], [24]. The present paper deals with steps 8-10.

The starting expander geometry equipped with supersonic nozzle blades is shown in Fig. 4, where a 3D view of the full geometry is illustrated.

In [24] the results of CFD modelling activities both with air and R404a and the model validation by means of test results are reported and discussed.

Although the achieved results were very promising, some fluid dynamic critical aspects of the pioneering geometry have been highlighted. Nozzle blades are not able to accelerate the flow till the expected supersonic conditions: a shock wave occurs before exiting the passage reducing the absolute velocity module to subsonic values and, consequently, twisting too much the relative velocity direction at the rotor inlet section.

In order to reduce such a phenomenon a new set of nozzle vanes was designed (Fig. 5).

A O-H 3D computational mesh for the simulation of two stator vanes and three rotor blade passages was generated (Figs. 6 (a) and (b)). The number of passages was chosen to achieve a good pitch ratio (ratio of facing areas at the interface between rotor and stator domains). The structured mesh counts about 300000 nodes for the rotor passages and about 150000 for the stator ones. Overall mesh quality parameters (maximum and minimum face angles, edge length ratio, element volume size) were checked to provide a good accuracy and a reasonable convergence time. The domain was extended in front of stator vanes and beyond the rotor exit section of a distance equivalent to one rotor inlet diameter in order to allow a fully developed flow entering the machine. At the interface between stator vanes and rotor blades a frozen rotor interface was set. Steady-state 3D viscous flow simulations were set up using a high-resolution advection scheme for the discretization of Navier-Stokes equations. In order to achieve preliminary information on the prototype capabilities a standard k-ε model with scalable wall function was selected.

To describe the refrigerant, the real gas cubic equation Aungier Redlich Kwong Model was chosen [25]. Such a model provides a reasonable prediction of the real fluid behavior in the cases of interest. The model is based on the equation of state written as:

$$p = \frac{RT}{v-b+c} - \frac{a(T)}{v(v+b)} \tag{4}$$

$$a = a_0 \left(\frac{T}{T_c}\right)^{-n} \tag{5}$$

$$a_0 = \frac{0.42747\, R^2 T_c^2}{p_c} \tag{6}$$

$$n = 0.4986 + 1.1735\, \omega + 0.4754\omega^2 \tag{7}$$

$$b = \frac{0.08664\, R\, T_c}{p_c} \tag{8}$$

$$c = \frac{R\, T_c}{p_c + \frac{a_0}{v_c\,(v_c+b)}} + b - v_c \tag{9}$$

being ω, Tc and pc the acentric factor and the critical temperature and critical pressure of the three pure R404a components (R125, R134a and R143a) respectively.

Three rotational speeds (30000, 60000 and 90000 rpm) have been taken into account. The total inlet pressure and temperature, the inlet velocity direction and the static pressure at the exit have been specified.

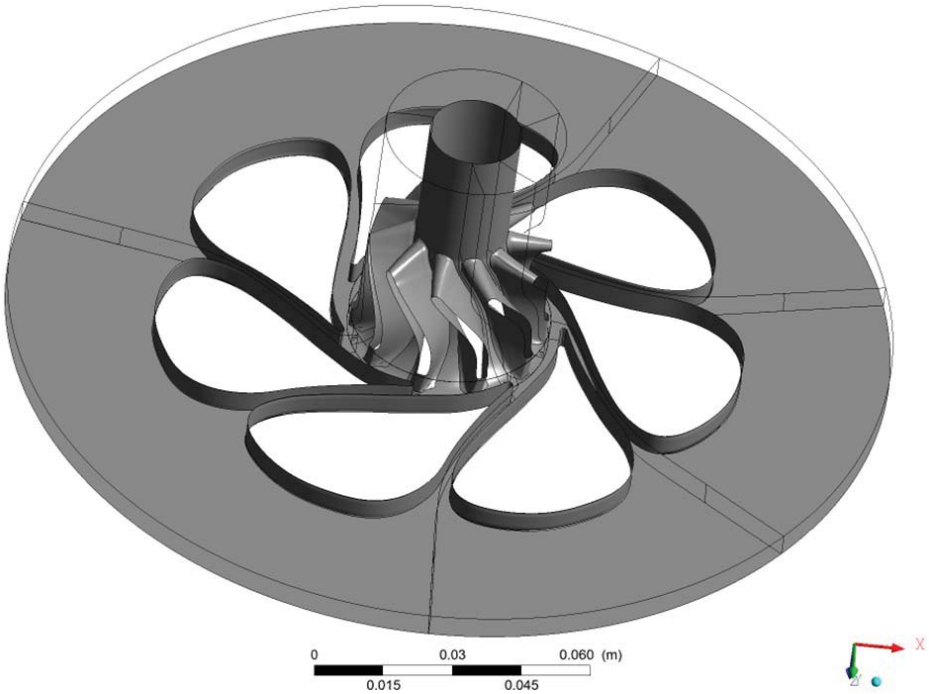

Fig. 4 CEG Expender old geometry

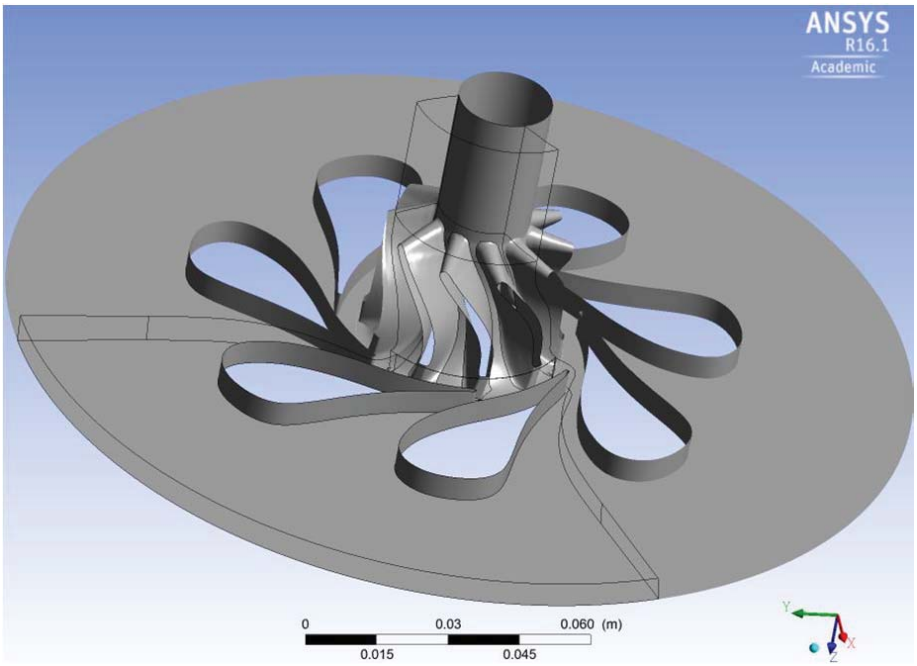

Fig. 5 CEG Expender new geometry

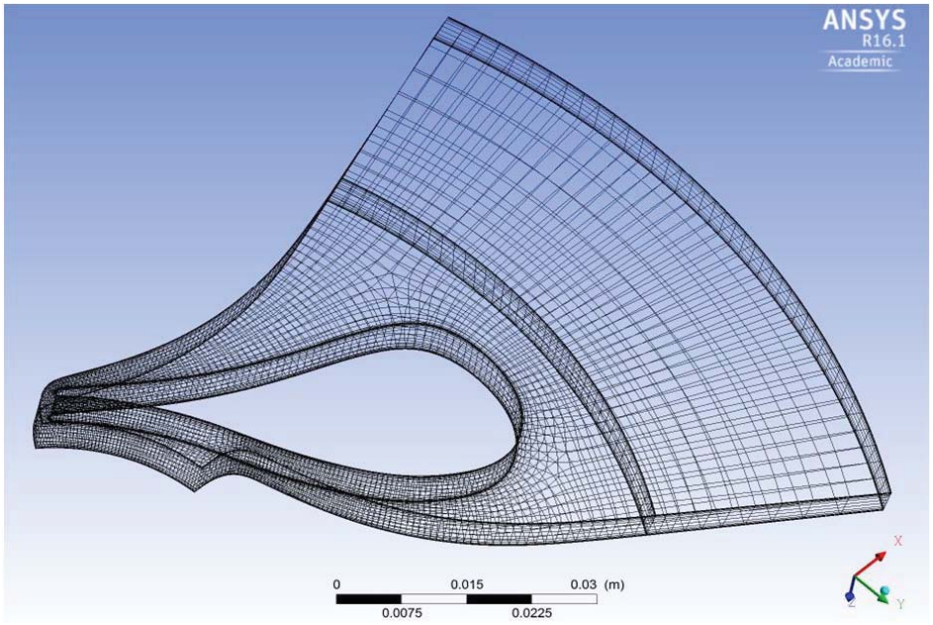

Fig. 6 (a) 3D view of O-H grids for a nozzle blade (new geometry)

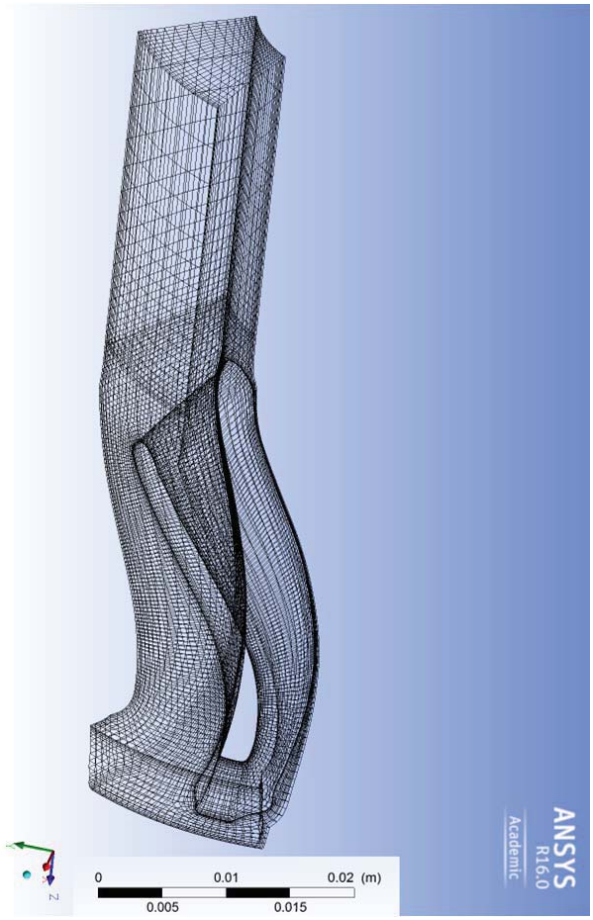

Fig. 6 (b) 3D view of O-H grids for a rotor blade

In Figs. 9-12 performance characteristics related to the new prototype geometry (Fig. 5) are reported. In particular, two different spacing between nozzle vanes and rotor blades have been simulated in order to evaluate the relevance of such geometric parameter on the fluid dynamic interaction between fixed and moving channels. Figs. 9 and 11 show the pressure ratio versus the mass flow, while Figs. 10 and 12 show the isentropic efficiency as function of the pressure ratio. The isentropic efficiency is defined as:

$$\eta = \frac{h_{Tin} - h_{Tout}}{h_{Tin} - h_{T\,is\,out}} \quad (10)$$

being h_{Tin}, h_{Tout} the total average enthalpies at the inlet and outlet section, respectively, and h_{Tisout} the isentropic total enthalpy at the rotor outlet section.

Comparing the achieved results with the performance of the first prototype at design opening, reported in Figs. 7 and 8, it is possible to highlight a significant improvement in the expander efficiency, especially for the second configuration (Figs. 11 and 12). The new nozzle geometry accelerates correctly the flow which has a post-expansion at the nozzle exit, before entering the rotor. No shock waves can be detected in the nozzles as in the old expander configuration. Nevertheless, modification in rotor blade shape are still required in order to reduce the wide stall region inside the rotor channels, which is still present as shown by the Mach number contour at mid-span of the new geometry in Figs. 14 and 15.

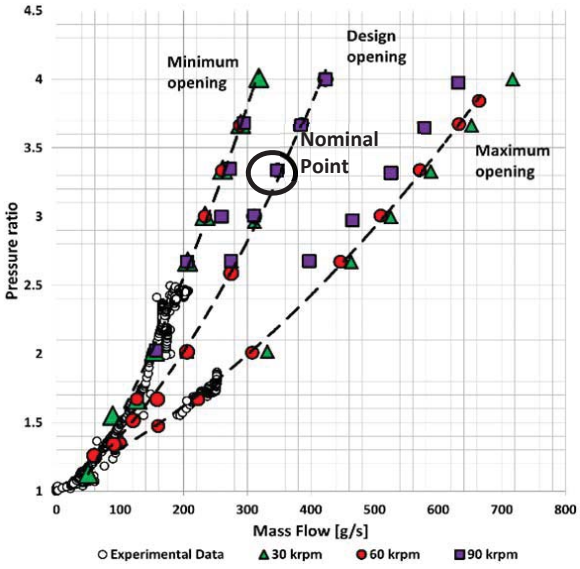

Fig. 7 Old expander characteristics: pressure ratio vs. mass flow

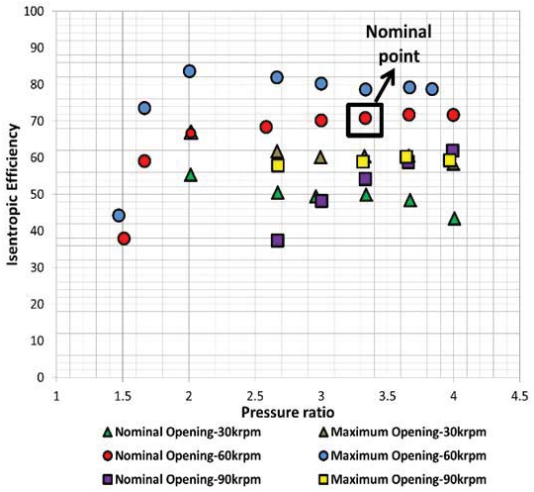

Fig. 8 Old expander characteristics: isentropic efficiency vs. pressure ratio

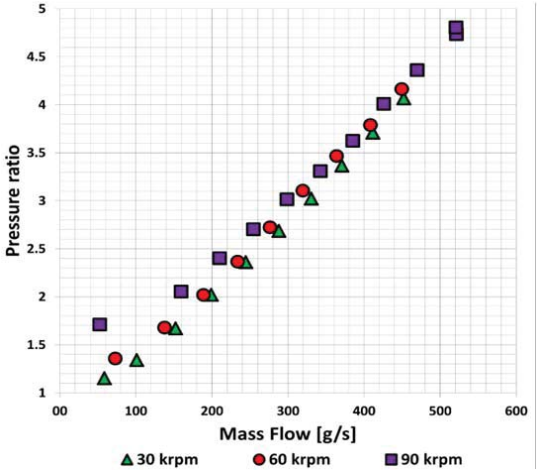

Fig. 9 New expander (n.1) characteristics: pressure ratio vs. mass flow

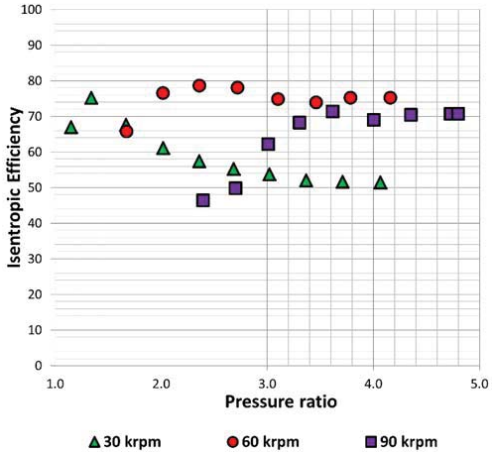

Fig. 10 New expander (n.1) characteristics: isentropic efficiency vs. pressure ratio

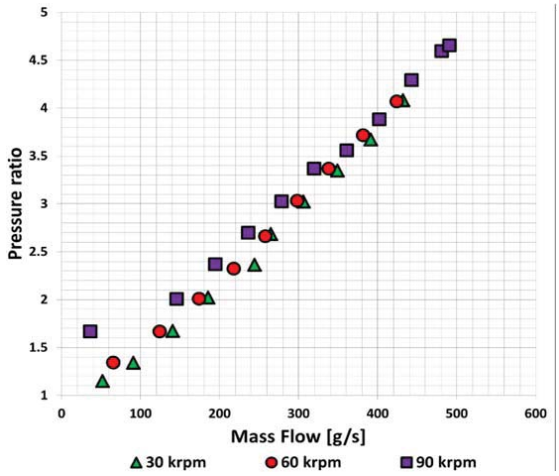

Fig. 11 New expander (n.2) characteristics: pressure ratio vs. mass flow

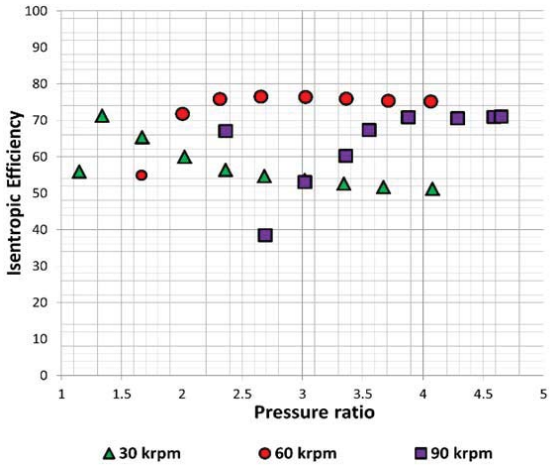

Fig. 12 New expander (n.2) characteristics: isentropic efficiency vs. pressure ratio

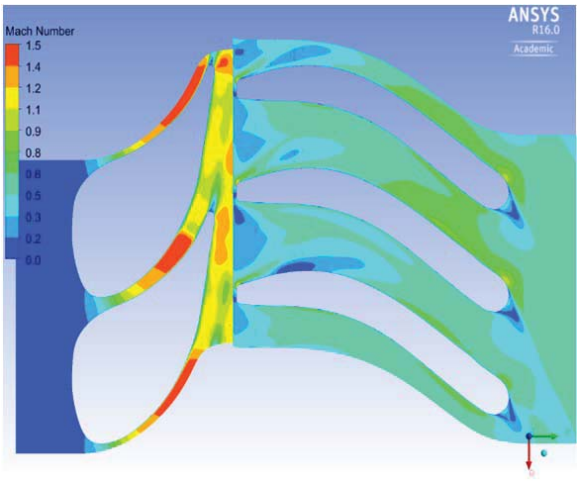

Fig. 13 Old geometry 60krpm Mach number contour on mid-span surface

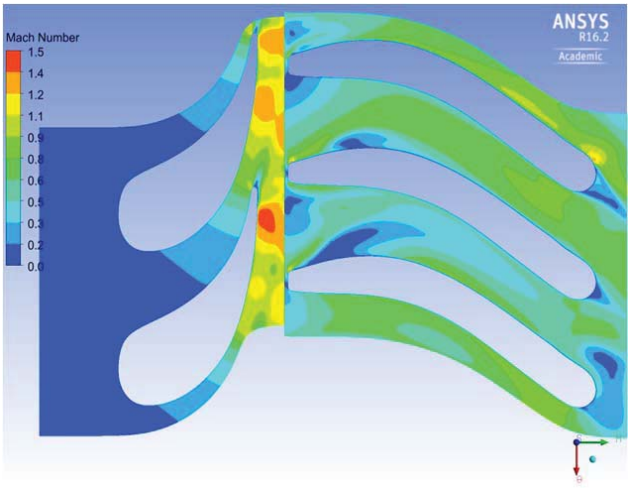

Fig. 14 New geometry (n.1) 60krpm Mach number contour on mid-span surface

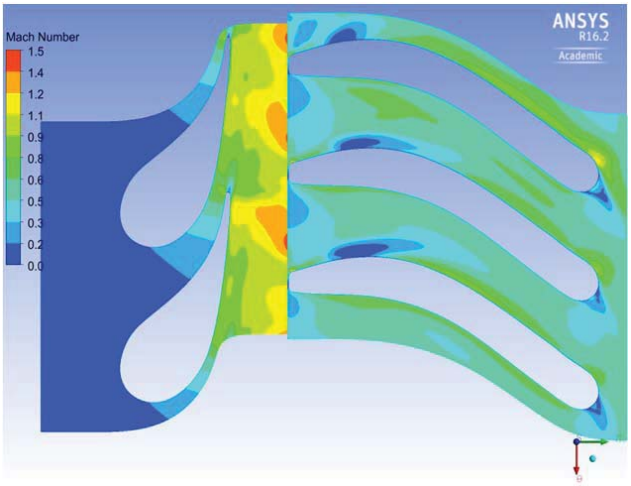

Fig. 15 New geometry (n.2) 60krpm Mach number contour on mid-span surface

V. Conclusions

This paper presents CFD modelling results for the performance evaluation of a second-generation expander prototype developed for an internal recovery system in VCR industrial plants.

The 3D model had been validated by means of experimental results in a previous work related to the analysis of the first-generation prototype.

Modifications to the nozzle shape had led to significant performance improvements in the expected nominal and off-design conditions. Moreover, comparing different gaps between the nozzle and rotor blades an improvement of the fluid dynamic conditions can be detected moving the nozzle away from the rotor inlet section. Nevertheless, further investigations are necessary to improve the rotor behavior, avoiding the stall detected in the rotor channels. Such a rotor blade optimization will be addressed in the future.

ACKNOWLEDGMENT

Authors acknowledge the Italian Ministry for the Environment, Land and Sea, Angelantoni Industrie S.p.A., SETEL S.r.l. and Roma Tre University for their support to the COLD-ENERGY Project.

REFERENCES

[1] S. Devotta, S. Sicars, IPCC/TEAP Special Report: Safeguarding the Ozone Layer and the Global Climate System, Chap. 4 – Refrigeration, Cambridge University Press, 2005.
[2] Arnemann M., Energy efficiency of refrigeration systems, International Refrigeration and Air Conditioning Conference, Paper 1356, 16-19 July 2012, West Lafayette (USA).
[3] Borlein C., Energy savings in commercial refrigeration equipment: Low pressure control, Schneider Electric White paper, August 2011.
[4] Yin X, Li S., Zheng Y., Cai W., Energy-saving-oriented control strategy for vapor compression refrigeration cycle systems, ICIEA 9th Conference on Industrial Electronics and Applications IEEE 2014.
[5] P. D. Gaspar, P. D. da Silva, Handbook of Research on Advances and Applications in Refrigeration Systems and Technologies, Engineering Science Reference, 2015.
[6] J. Sarkar, Ejector Enhanced Vapor Compression Refrigeration and Heat Pump Systems - A Review, *Renewable and Sustainable Energy Reviews* 16, 6647-6659; 2012
[7] Widell K.N., Eikevik T., Reducing power consumption in multi-compressor refrigeratopn systems, International Journal of refrigeration, Vol. 33, 88-94, 2010.
[8] Joost J. Brasz, Carrier Corporation, Refrigeration apparatus with expansion turbine, European patent EP 0 676 600 B1, September 6, 2000.
[9] F.L. Goldsberry, Refrigerant expander compressor, US Patent, 3 932 159, Jan 13, 1976.
[10] D.A. Ritchie, Energy covery system for refrigeration systems, US Patent, 4 141 222, Feb. 27, 1979.
[11] W.T. Osborne, Refrigeration system with turbine drive for compressor, US Patent 3 276 226, Oct. 4, 1966.
[12] B. Mitra, Y.H. Chen, Refrigerant vapor compression system with dual economizer circuits, International application published under the patent cooperation treaty (PCT), WO 2008/130359 A1, 30 Oct. 2008;
[13] B. Mitra, Y.H. Chen, Refrigerant vapor compressin system with flash tank economizer, International application published under the patent cooperation treaty (PCT), WO 2008/140454 A1, 20 Nov. 2008.
[14] F. T. Abdelmalek, Centrifugal gas compressor expander for refrigeration, US Patent 5 136 854, Aug 11, 1992.
[15] S. Ro, Refrigeration apparatus with turbo compressor, US Patent, 7 451 616, Nov. 18, 2008.
[16] T. J. Leck, D.B. Bivens, F. Zhao, M. Rohacek, Refrigeration/air conditioning apparatus powered by an engine exhaust gas driven turbine, US Patent, 2006/0242985 A1, Nov. 2, 2006.
[17] M. Ascani, Refrigerating Device and Method for Circulating a Refrigerating Fluid Associated with it, *United States Patent*; Patent No.: Us 8,505,317 B2; Aug.13, 2013.
[18] Cerri G., Alavi S. B., Chennaoui L., Giovannelli A., Mazzoni S., Optimum turbomachine selection for power regeneration in vapor compression cool production plants, International Journal of Mechanical, Aerospace, Industrial and Mechatronics Engineering Vol. 9, No. 4, 2015.
[19] Archilei E. M., Expander Compressor Goup for energy saving in cryogenic plants, Master Thesis, 2012.
[20] COLD-ENERGY Technical Report OR3-A3, Design, CEG prototype, Test bench, 2014.
[21] S.L. Dixon, CA. Hall, Fluid Mechanics and Thermodynamics of Turbomachinery, *Butterworth Heinemann*, Sixth Edition, 2010.
[22] O.E. Baljè, Turbomachines: A Guide to Design, Selection, and Theory, *John Wiley and Sons*, New York; 1980.
[23] NIST Reference Fluid Thermodynamic and Transport Properties – REFPROP Version 7.0.
[24] A. Giovannelli, E.M. Archilei, Design of an expander for internal power recovery in cryogenic cooling plants, Energy Procedia, Vol. 82; Dec 2015, pp. 180-185.
[25] Aungier R.H., A fast, accurate gas equation of state for fluid dynamic analysis applications, Journal of Fluid Engineering, Vol. 117, p. 277–281, 1995.